Structure-function relationship between preferred orientation of crystallites and electrical resistivity in thin polycrystalline ZnO:Al films

M. Birkholz
Fraunhofer Institut für Schicht- und Oberflächentechnik, Bienroder Weg 54 E, 38108 Braunschweig, Germany

B. Selle, F. Fenske, and W. Fuhs
Hahn-Meitner-Institut, Silizium Photovoltaik, Kekuléstr. 5, 12489 Berlin, Germany

(Received 2 April 2003; revised manuscript received 28 May 2003; published 18 November 2003)

Thin polycrystalline films are often observed to develop a preferred orientation or texture that may have significant effects on film properties, especially in the case of anisotropic crystal structures. We report on a x-ray diffraction study of texture evolution in hexagonal ZnO:Al films, which were performed with a highly sensitive large-area detector enabling the investigation of films with thicknesses of some 10 nm only. In a set of magnetron-sputtered ZnO:Al films with thicknesses between 20 and 500 nm the resistivity was found to decrease with increasing thickness. A comprehensive texture analysis was performed within the framework of the series expansion method of the orientation distribution function (ODF). The investigations reveal a clear correlation between preferred grain orientation and electrical properties in ZnO:Al films. A general model is presented which relates the electronic mobility in polycrystalline films with the ODF by assuming the mobility to be composed of an intra-grain and an inter-grain fraction. It turns out that intra-grain anisotropy in ZnO:Al films cannot account for the observed variations in resistivity. Regarding the charge carrier scattering at grain boundaries the model relates the resistivity to the degree of grain alignment and makes use of the texture index J. On the basis of these assumptions it is shown that the resistivity scales with $1/J$. The model also predicts the attainable minimum resistivity of thin ZnO:Al films with perfectly aligned crystallites which is in accordance with previously published results.

DOI: 10.1103/PhysRevB.68.205414 PACS number(s): 68.55.Jk, 61.10.Nz, 73.50.−h, 73.61.Ga

INTRODUCTION

The properties of polycrystalline materials are strongly determined by structural and morphological parameters of the grain population.[1] Therefore, an interpretation of properties of thin polycrystalline films often faces the problem of averaging over a large number of crystallites, the orientation distribution function (ODF) of which might significantly affect film properties. The effect of averaging becomes especially important if the coating material exhibits an anisotropic crystal structure or in the case of electronic properties of thin films, for which applications very often require a high in- plane mobility of electronic charge carriers. Thin polycrystalline zinc oxide films represent a material system for which both effects may be relevant. Such films are of technical importance for surface acoustic devices, sensors, catalysts and—by doping with aluminum—as transparent conductive oxides in solar cells, thin film transistors for flat panel displays.[2] Thin ZnO and ZnO:Al films generally exhibit the hexagonal wurtzite structure, space group $P6_3mc$, with unit cell lengths $a=325.0$ pm and $c/a=1.602$; see Ref. 3 for a review on the physical properties of ZnO and other II-VI compounds. It was often reported in the literature that thin films show a preferred orientation of grains having the crystallographic c axis oriented parallel to the substrate normal. This phenomenon was found to occur for a large variety of different deposition conditions like dc and rf magnetron sputtering,[4–9] pulsed laser deposition,[10] and metal-organic chemical vapor deposition.[11,12] Since the preferred orientation of crystallites seemed to be correlated with an increase of electrical conductivity of ZnO:Al films, this structural property appeared as one of the key parameters for the preparation of highly transparent layers with optimized conductivity.

The goal of this work was to investigate the relationship between texture and resistivity for a series of dc magnetron sputtered ZnO:Al samples. Many previous works on this issue focused on the size of ZnO grains in the film as the structural quantity which strongly influences the electronic properties. Here, a new approach will be introduced by considering the preferred orientation of crystalline grains. We think that both structural quantities—size and texture—are determining the electronic mobility. In the present work the focus is on the influence of texture. In the recent years x-ray diffraction techniques for the determination of textures were introduced into the field of thin film analysis that, so far, have been applied for the investigation of bulk samples, mostly consisting of one-elemental metals or alloys.[1,13] A widely used method for the investigation of thin film texture is the determination of a so-called texture factor which derives from the ratio of peak intensities that are related to the expected values as determined for randomly oriented crystallites in a powder.[14–16] However, a complete texture determination of compound thin films has been performed in only a few cases, because of difficulties in the measurement of low scattering intensities. These experimental restrictions were meanwhile overcome by the introduction of large-area detectors for laboratory x-ray sources. In this work we evaluate the applicability and efficiency of these techniques for the investigation of thin solid films with the aim to derive the relationship between structure and functional properties for a transparent conductive oxide.

TABLE I. C_l^μ coefficients of ODF expansion for all investigated samples. Columns are ordered according to the nominal thickness d of ZnO:Al layers as given in the head line. The last lines list the texture index J and resistivity ρ.

d/nm	25	40	70	100	150	200	300	500
$(l,\ \mu)$								
(2,1)	0.552	0.617	0.555	0.861	1.584	1.511	1.362	2.143
(4,1)	−0.066	−0.002	−0.115	0.319	1.123	1.491	1.384	2.290
(6,1)	0.071	0.067	0.331	0.140	0.310	0.990	0.931	1.157
(6,2)	−0.103	−0.106	0.153	−0.065	0.340	0.294	0.153	0.442
(8,1)	0.569	0.558	0.469	0.573	0.555	0.970	0.193	0.766
(8,2)	0.225	0.148	0.136	0.195	0.327	0.365	−0.250	0.471
(10,1)	−0.121	−0.129	−0.254	−0.142	−0.045	0.207	0.309	0.029
(10,2)	−0.285	−0.429	−0.574	−0.391	−0.383	−0.063	0.310	−0.173
(12,1)	0.074	0.069	0.328	0.088	0.163	0.335	0.084	0.301
(12,2)	−0.428	−0.117	−0.537	−0.335	0.262	−0.618	−0.303	0.038
(12,3)	−0.043	0.160	−0.122	−0.011	0.301	−0.279	−0.449	−0.006
(14,1)	−0.199	−0.214	−0.352	−0.265	−0.243	−0.078	0.262	0.112
(14,2)	−0.703	−1.030	−0.761	−0.762	−0.629	−0.588	0.388	−0.484
(14,3)	−0.001	−0.051	0.022	0.063	0.093	0.063	−0.174	−0.097
J	1.12	1.17	1.18	1.17	1.41	1.61	1.44	2.00
$\rho/10^{-3}\ \Omega$ cm	14	12	10	6.7	6.6	5.1	4.1	3.7

EXPERIMENT

A series of ZnO:Al samples was prepared by reactive dc magnetron sputtering from a metallic Zn-Al (2 wt %) alloy target of 99.99% purity and 90 mm diameter. The planar sputtering source was placed parallel to the substrate holder in sputter-up configuration with a target-to-substrate distance of 55 mm. All depositions were carried out on stationary substrates, which were neither intentionally heated nor biased. High purity 6N argon and oxygen were used as process gases. Inside the deposition chamber the gas flow was directed to the discharge zone by a ring tube with small orifices. Setting a constant oxygen flow rate the total pressure was held constant at 0.6 Pa by adjusting the Ar flow rate. The high pumping speed of the unthrottled system preserved low gaseous contaminants during the deposition process and prevented reactive gas pressure instabilities. After evacuating to a pressure of less than 10^{-5} Pa the target was presputter cleaned until the cathode voltage equilibrium value of the poisoned, i.e., the oxide-covered target, was obtained. The target was sputtered in the constant-power mode with 100 W. These deposition conditions were identified in previous studies to yield highly transparent ZnO:Al films with the lowest resistivities[17] compared to samples which were prepared under variations of the argon content or oxygen flow.[6]

Thin ZnO:Al films were deposited on Si wafers coated with about 400-nm standard thermal SiO_2 for electrical insulation. Four point probe measurements were performed at room temperature to determine the sheet resistance. A nominal thickness of films was calculated from the deposition time and deposition rate, which was found in a preceding experiment to amount to 1.1 nm/s under the process conditions given above. The resistivities of all samples are compiled in Table I. Further details of sample preparation and characterization of their composition, structure, optical and other properties can be found in Ref. 18.

ZnO:Al films deposited at room-temperature conditions by PVD processes were found in many investigations to exhibit the morphological properties of structure zone T as introduced by Thornton into the structure zone model (SZM).[19–21] The homologous temperature T_s/T_m, which is the ratio of substrate temperature T_s and melting temperature T_m, is about 0.2 in our experiments at 300 K. T_s/T_m is accordingly at the lower end of values for which zone T is generally observed, i.e., $0.2 < T_s/T_m < 0.4$. It has to be taken into account that the effective deposition temperature might be enhanced due to the interaction of the growing film with the plasma. Also in our previous investigations[22] the typical growth morphology of zone T could be identified to occur in the films as investigated in this work. Zone T is associated with an evolutionary development of texture with increasing thickness, where—in the cases of ZnO and ZnO:Al—(00.1)-oriented grains grow on the expense of other orientations. Due to the thickness dependence of the texture evolution process we applied a texture engineering in terms of the SZM by simply varying the deposition time and leaving all other deposition parameters unchanged. Eight samples were prepared exhibiting a nominal thicknesses of 25, 40, 70, 100, 150, 200, 300, and 500 nm. By virtue of this method we have prepared a set of samples with different texture.

Measurements of preferred orientation were performed with a Bruker AXS General Area Detector Diffraction System (GADDS) equipped with a HI-STAR detector. The scattered x-ray photons were measured by virtue of a two-dimensional multiwire proportional counter with subsequent position decoding circuits leading to a 10^4-fold increased sensitivity in comparison to a conventional scintillation counter.[23] A significant advantage of this detector system for thin film work is the parallel acquisition of many scattering events on a large circular area with a diameter of 115 mm. The usage of such a high-sensitivity detector system was

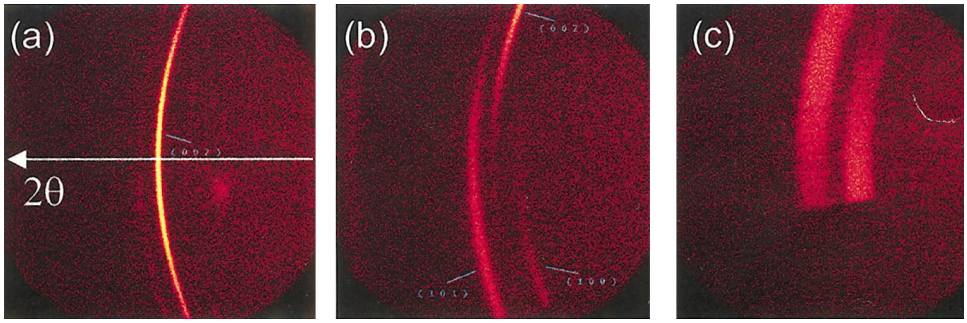

FIG. 1. (Color) Two-dimensional diffraction pattern of the thickest 500-nm ZnO:Al sample as measured with the HISTAR detector for tilting angles of (a) 0°, (b) 45° and (c) 80°. The arrow in (a) gives the path of a conventional θ-2θ scan pointing towards increasing scattering angles 2θ.

necessary in order to obtain reliable signal-to-noise ratios of Bragg reflections even for the thinnest samples within an acceptable amount of time.

A long fine focus Co tube was used as x-ray source (Co$K\overline{\alpha}$=179.03 pm) and operated in the spot focus mode with 50 kV and 30 mA. The elimination of the $K\beta$ line was performed by virtue of a graphite monochromator positioned between the x-ray tube and sample. The x-ray beam spot upon the sample was confined by a pinhole collimator to a diameter of 1 mm. The distance between the illuminated mid-point of the sample and detector was set to 150 mm. The height alignment of the sample on the goniometer head was performed with a laser-video microscope. A $\frac{1}{4}$ circle Eulerian cradle was applied for tilting the substrate normal out of the diffraction plane, while the position of the x-ray tube and the detector were kept constant. Because of the parallel acquisition of diffracted beam intensities by the two-dimensional HI-STAR detector, three diffraction patterns measured at tilt angles of 0°, 45°, and 80° were sufficient for the determination of the x-ray pole figures. It was thereby implicitly assumed that the preferred orientation of ZnO crystallites would be of rotational symmetry with respect to the substrate normal, which is called a fiber texture. The development of fiber textures is typically observed in thin films and may easily be understood from the fact that the substrate normal is the single extraordinary direction. The 200 nm thick sample was explicitly investigated with respect to a rotational texture symmetry by measuring various diffraction patterns under the same tilt angle. However, no statistically significant variations of the diffraction patterns could be identified for different angles of rotation within the sample plane. It was therefrom concluded that the assumption of rotational symmetry was indeed fulfilled.

Figure 1 displays the set of two-dimensional diffraction patterns as obtained for the thickest sample of a nominal thickness of 500 nm for three different tilt angles. Three Debye rings of ZnO Bragg reflections can clearly be identified, the intensities of which depend on orientation. These lines account—from right to left—for the (10.0), (00.2), and (10.1) reflections which appear in the case of Co$K\alpha$ radiation at scattering angles 2θ of 37.1°, 40.2°, and 42.4°. The usual, symmetrical 2θ scan in Bragg-Brentano geometry would correspond to a passage of a zero-dimensional detector along the center line given in Fig. 2(a). A weak reflection can be identified in the first pattern, accounting for the—forbidden, but for single-crystalline Si substrates generally observed—Si reflection of order (200). The preferred orientation of ZnO crystallites with the c axis aligned along the substrate normal may already be recognized from these raw data patterns: while the (00.2) reflection at $\psi=0°$ appears to be the strongest and sharpest of all observed reflections, it disappears for a tilt angle of 45° in the middle of the pattern and vanishes completely at 80°. On the other hand, in Fig. 1(c) the (10.0) and (10.1) rings have significantly gained intensities, which will partially stem from crystallites having their (00.2) direction close to the fiber axis ($\angle$) ($[(00.2),(10.0)]=90°$ and ($\angle$) $[(00.2),(10.1)]=58°$) from where they simple scatter in another diffraction order ($hk.\ell$). The decrease of intensity of the (00.2) ring towards the edges of diffraction pattern is not solely due to the preferred orientation effect, but also caused by defocusing, which the scattered radiation suffers with increasing tilt angle ψ.

Even for the thinnest sample of only 25 nm thickness a diffraction pattern was obtained after an integration time of only 600 s. For the tilt angle of 0° the (00.2) reflection was clearly recognized, indicating that at least a part of the deposited ZnO:Al has crystallized in the hexagonal wurtzite structure. It can be concluded from this observation that any possible amorphous boundary layer adjacent to the

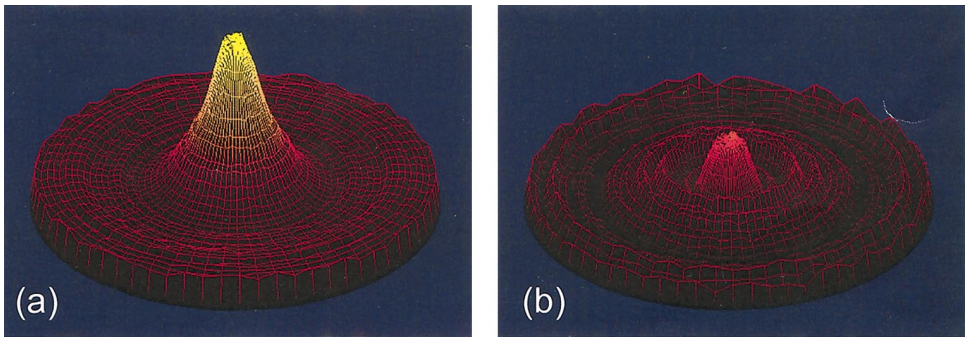

FIG. 2. (Color) Pole figures of the (a) thickest (500 nm) and (b) thinnest (25 nm) ZnO:Al samples, without absorption corrections.

substrate—as it occurs for instance during the growth of silicon films by chemical vapor deposition[24]—would have a thickness of significantly less than 25 nm.

It has to be emphasized that the detection of such low-intensity reflections would have been impossible without the superior sensitivity of the GADDS/HI-STAR system. In a conventional diffractometer system the Bragg reflection intensity is only collected in the scattering plane, which is defined by the position of the x-ray intensity centroids on the anode focus, the sample and the detector slit. In contrast, by usage of a two-dimensional detector, diffracted intensity is also measured at positions above and below the scattering plane. This measurement technique, however, does not rely on extending the primary beam path within the sample volume as it is used in grazing incidence techniques. Here, as in the usual symmetric θ-2θ diffractometer configuration, a large part of the primary intensity penetrates through the film into the substrate and is lost for delivering structural information about the thin film. Also with respect to these considerations, the total integration time for obtaining one diffraction pattern appears remarkably short.

METHOD OF ANALYSIS

Pole figures of (10.0), (00.2), and (10.1) reflections were derived simultaneously from the two-dimensional diffraction pattern as measured under tilt angles of 0°, 45° and 80° for each sample. Pole figures as measured in reflection geometry are always incomplete, since intensities close to tilt angle $\psi = 90°$ remain unmeasurable. Because of the hexagonal crystal symmetry of ZnO, the measurement of three nonharmonic reflections with an area detector under three tilt angles yielded sufficient information for the complete solution of the texture problem. Figure 2 displays the uncorrected pole figures of (00.2) reflections for the thickest and thinnest ZnO:Al films. The defocussing effects, which can be seen in Fig. 1 to increase with increasing tilt angle, were automatically corrected during the computer-based analysis of raw data.[25] A further correction was necessary because of the finite sample thickness, since the integrated intensity of a thin-film Bragg reflection is damped by the sample thickness factor A,[26] which reads, for a reflection at 2θ and tilt angle ψ,

$$A = 1 - \exp(-2\mu d/\sin\theta\cos\psi). \tag{1}$$

Here μ denotes the absorption coefficient of ZnO, which for Co$K\alpha$ radiation amounts to $\mu = 417.2\ \mathrm{cm}^{-1}$ as calculated from $\mu_{\mathrm{Zn}} = 87.1$, $\mu_{\mathrm{O}} = 18\ \mathrm{cm}^2/\mathrm{g}$[27] and an x-ray density of $\rho_{\mathrm{ZnO}} = 5.675\ \mathrm{g/cm}^3$ (Ref. 3) (the usage of symbol μ in this context should not be confused with the mobility of electric charge carriers as discussed in subsequent sections of this work). As-measured intensities were also corrected with respect to the finite sample thickness.

The solution of the texture problem can be represented by the orientation distribution function ODF, which describes the distribution of crystallites' orientations in the orientation space. In the case of a rotational symmetric texture the orientation of crystallites can be specified by only two of generally three Euler angles (Φ,β) that account for the inclination and rotation of the crystallite coordinate system K_B with respect to the sample coordinate system K_A. We choose the surface normal as the z axis of K_A, while the x and y axes may be arbitrarily defined in the film plane. Regarding the crystallite coordinate system K_B, the (00.1) direction was selected as z the axis, while x and y were chosen to lie along the a and b edges of the hexagonal unit cell. This setting is the most appropriate for the texture geometry of the investigated samples. The ODF for fiber textures $R(\Phi,\beta)$ is described by a linear combination of normalized spherical surface harmonics k_l^μ weighted by coefficients C_l^μ

$$R(\Phi,\beta) = \sum_{l=0(2)}^{l_{\max}} \sum_{\mu=1}^{M(l)} C_l^\mu k_l^\mu(\Phi,\beta). \tag{2}$$

The summation is restricted to even l values only. For the analysis presented in this work the sum was limited to $l_{max} = 14$, which in many previous texture investigations turned out to be associated with negligible truncation errors. The possible number of coefficients is moreover reduced by geometrical constraints due to the crystal symmetry. In the case of a wurtzite structure ZnO, the hexagonal symmetry led to $M(l) = 1$, 2, and 3 for $l = 2$, 4, or 6, 8, 10 and 12, 14, respectively. The basis functions k_l^μ are defined through

$$k_l^\mu = \frac{1}{\sqrt{2\pi}} \begin{cases} \overline{P}_l(\cos\Phi), & \mu = 1 \\ \sqrt{2}\cos(6\mu\beta)\overline{P}_l^{6\mu}(\cos\Phi) & \mu > 1, \end{cases} \tag{3}$$

which can be derived by applying the symmetry elements of the hexagonal symmetry groups to the general ODF basis functions.[1,28] $\overline{P}_l$ and $\overline{P}_l^\mu$ account for normalized Legendre functions and associated Legendre functions, respectively. The solution of the texture problem consisted of the evaluation of all coefficients C_l^μ from the measured pole figures, for which purpose the least square method for incomplete pole figures as given in the literature was applied.[1] Finally, it is realized that $14 C_l^\mu$ values have to be determined and this number decomposes into two times seven coefficients, for which either $\mu = 1$ or $\mu \neq 1$ holds. The sum of all squares of C_l^μ coefficients,

$$J = \frac{1}{4\pi} \sum_{l,\mu} [C_l^\mu]^2, \tag{4}$$

is called texture index. In case of a random orientation distribution one has $J = 1$ and all C_l^μ vanish, except for the first one which is set to $C_0^1 = \sqrt{4\pi}$ in order to realize a normalization. The texture index increases with increasing preferred orientation and represents a measure of the texture's sharpness. C coefficients and texture index J were computed from the three measured pole figures by virtue of the TexEval program.[25]

In x-ray diffraction (XRD) the integrated intensity of Bragg reflexes scales with the volume density of those crystallite grains which actually scatter into the detector. The XRD-determined ODF therefore accounts for the volume share of the sample, which can be assigned to the appropriate infinitesimal element in orientation space, i.e., within the formalism used here the ODF is defined by

$$\frac{dV(\Phi,\beta)}{V} = R(\Phi,\beta)\sin\Phi d\beta d\Phi. \quad (5)$$

By integrating the ODF in Euler space one therefore obtains a volume average of orientations.

RESULTS AND DISCUSSION

In Table I all 14 C_l^{μ} coefficients are listed for each of the investigated samples. The table also gives the texture index J as calculated from C_l^{μ} coefficients. J can be seen to increase from 1.12 to 2.00 with increasing film thickness. Even for the thinnest sample of only 25 nm thickness the texture index is larger than 1, i.e., a preferred orientation of c-axis-oriented crystallites has already started to overgrow any random orientation. Moreover, it can be concluded that the intended texture variation by varying the deposition time has indeed successfully been performed.

This result clearly indicates that the increase of the film thickness d and the decrease of the film resistivity ρ are correlated with an enhancement of (00.1) preferred oriented grains. The increase of the texture is a competitive process, since the growth of c-axis-oriented grains occurs at the expense of other crystallographic directions. A small value for the resistivity ρ of Al-doped ZnO thin films is often indicated as a quality parameter for the deposition process. It is evident from the presented results, however, that such a parameter is of little significance if the film thickness is not specified, too. The literature on thin ZnO:Al films gives numerous hints that many other groups have been preparing films with a competitive (00.1) texture, which will have also been associated with a decrease of resistivity.

The mobility of electronic charge carriers in ZnO:Al of optimized conductivity at room temperature is determined by their scattering at ionized impurities and phonons, while other factors may be neglected in the high doping regime. A review of the material's electronic resistivity including an estimation of the physical limit of minimum resistivity has recently been given by Ellmer.[29] In the following the relationship between electrical conductivity and the structure of ZnO:Al films will be discussed in some more detail. As has already been mentioned, the consideration of the influence of grain size will be neglected. It has to emphasized that the thorough investigation of grain sizes and its influence on film conductivity should include the measurement of in-plane grain sizes, which lies beyond the scope of this work.

The following part of the discussion should be considered as an example for an investigation of a special case of orientational averaging for which the set of C_l^{μ} coefficients will be tested in order to achieve a quantitative understanding of the electronic properties of polycrystalline ZnO:Al films. For this purpose, it will be assumed, firstly, that the anisotropy of charge carrier mobility within single grains may affect the conductivity and, secondly, that the electronic transport between two grains across grain boundaries may exhibit a pronounced dependence on orientation. The latter effect has been studied extensively in the case of silicon, where large-angle grain boundaries were found to significantly deteriorate the electrical properties of polycrystalline thin films. The basic approach therefore was to split the conductivity into an intra-grain fraction σ_{intra} and an inter-grain fraction σ_{inter}, the sum of which yields the measured quantity. Both mechanisms are visualized in Fig. 3.

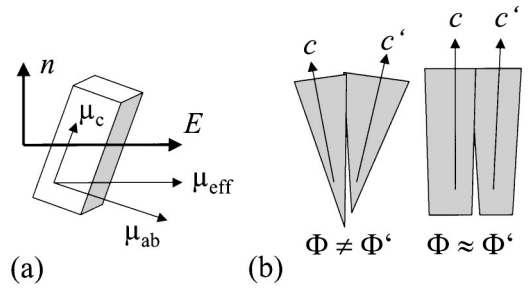

FIG. 3. Modeling of the two mechanisms that might determine the electrical resistivity in polycrystalline thin films via (a) intragrain and (b) intergrain mobility effects. n gives the direction of the substrate normal, perpendicular to which the electrical field E is applied. The electronic mobility in hexagonal crystals splits into two contributions μ_{ab} and μ_c. The average value μ_{eff} depends on the relative orientation between c axis and substrate normal.

Regarding the anisotropic transport within single grains it is well known for ZnO that a piezoelectric scattering is active in addition to the usual scattering components due to phonons and ionized impurities. However, the piezoelectric scattering mechanism acts only in the direction of the hexagonal c axis, thereby causing a reduction of the carrier mobility by a factor of about 2 compared to the value in the ab plane.[30] An anisotropic component of the mobility will occur in Al-doped material, too, since the Al doping does not alter the anisotropic structure of the crystallographic unit cell. By considering this approach we are aware of the fact that according to recent publications[17,29] the electronic mobility in ZnO:Al in the high doping regime is mainly influenced by ionized impurity scattering, $\mu \approx \mu_{\text{ii}}$. Due to the reciprocal addition of mobilites via Matthiesen's rule, μ_{ii} will probably dominate over all other factors that may affect the total mobility. The following considerations should therefore be taken as a model study for investigating the relation between preferred orientation and electronic conduction in anisotropic polycrystals.

One may imagine that because of the large number of grains that have to be traversed by the charge carriers in the plane of the film, the resistivity increases with an increase in the preferred orientation along the fiber axis, since the electronic transport then occurs mostly within the basal ab plane of the hexagonal unit cell. This would be associated with a reduced total scattering of charge carriers leading to enhanced conductivity; see Fig. 3. This fraction is related to an intragrain effect of mobility and can be represented by the ansatz

$$\mu_{\text{intra}} = \mu_{ab}\cos^2\Phi + \mu_c \sin^2\Phi \quad (6)$$

where Φ is the angle between the c axis of an individual crystallite and the substrate normal. The average intragrain mobility $\mu_{\text{av,intra}}$ can quantitatively be evaluated on the basis of the ODF by integrating over all different orientations and weighting with the appropriate mobility. Since the XRD-

determined ODF measures volume fractions [see Eq. (5)], the intragrain averaged mobility turns out to be proportional to

$$\mu_{ab}\int (\cos^2\Phi + r\sin^2\Phi)R(\Phi,\beta)\sin\Phi d\beta d\Phi, \qquad (7)$$

with r giving the ratio of μ_c and μ_{ab}. The integral was solved for each sample on the basis of the ODF given in Eq. (2). It was thereby assumed that the intragrain mobility is not affected by the rotation angle β. Interestingly, it was found that neither the parallel-ab nor parallel-c mobility was significantly affected by the variation of the ODF of ZnO:Al grains—which holds for reliable values of r, especially for $r=\frac{1}{2}$. For this special case $\mu_{\mathrm{av,intra}}$ varied only by about 12% when calculated with the eight sets of C_l^{μ} coefficients given in Table I. We therefore conclude that the intragrain anisotropy of charge carrier transport cannot account for the observed increase in conductivity by about 380% with increasing texture. This result would not only hold for piezoelectric scattering, but is valid irrespectively of what physical mechanism might cause the anisotropy of intra-grain mobility.

Second, the increased density of (00.1)-oriented crystallites in a thin ZnO:Al layer is associated with a reduction of large-angle grain boundaries. Instead, the density of small-angle grain boundaries increases, which are known to be associated with a smaller density of electronic defects and of active scattering centers for charge carriers. In the framework of this argument it is therefore assumed that the transport of charge carriers is the less affected by grain boundary scattering the smaller the orientation distance between the two grains becomes. Accordingly, for two grains with orientations (Φ,β) and $(\Phi+\Delta\Phi,\beta+\Delta\beta)$, the intergrain mobility will decrease with an increasing orientation difference $(\Delta\Phi,\Delta\beta)$. For a complete quantitative formulation of this approach one would rely on a precise knowledge of the intergrain mobility versus $(\Delta\Phi,\Delta\beta)$. Although, some special cases of intergrain mobility in ZnO have already been investigated, for Sb-doped ZnO for varistor applications (see for instance, Ref. 31), the data set is still far from being complete. One therefore has to use a practical approximation for a quantitative formulation of the intergrain mobility. For this purpose it is realized that the electronic transport would remain ideally unaffected between two perfectly aligned crystallites having $\Delta\Phi=\Delta\beta=0$. The probability for the volume density of such configurations is $R(\Phi,\beta)^2$, while the averaging over the total grain population affords the integration over all such configurations. We therefore consider the expression

$$\int [R(\Phi,\beta)]^2\sin\Phi d\beta d\Phi = J \qquad (8)$$

as a measure for the degree of grain alignment within the polycrystal. It is shown by texture theory[1] that this integral equals the texture index J as given in Eq. (4) because of the orthonormality of the k_l^{μ} basis function; see Eq. (3). The texture index J is 1 for a random grain orientation and diverges to infinity for a single crystallite. Considering the $1/J$ axis these two extremes are found at 1 and 0. It is evident from these two extreme cases that the conductivity σ would scale with J, while the resistivity ρ would scale with $1/J$.

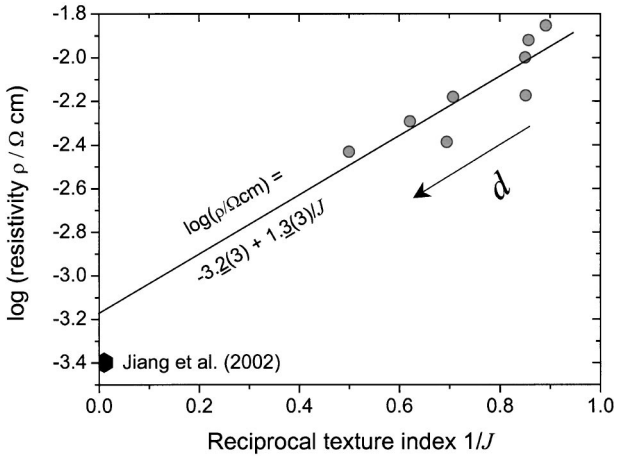

FIG. 4. Plot of $\log(\rho/\Omega\mathrm{cm})$ versus reciprocal texture index $1/J$ for all investigated ZnO:Al samples. Gray dots account for thin film investigated in this work. The black hexagon should indicate the samples due to Ref. 8, where a self-texture growth mechanism was obtained, which is assumed here to have a $1/J$ close to 0.

In Fig. 4 the dependence of $\log(\rho/\Omega\mathrm{cm})$ versus $1/J$ is shown. This mathematical form of the interdependence between ρ and J was chosen in order to account for the effect of a very large number of grain boundaries that have to be crossed by charge carriers. The direction of increasing film thickness is indicated in the figure to decrease along the chosen abscissa. A linear regression of the data with the model formula $\rho=A\exp(B/J)$ was performed with A and B as fit parameters and the solution is given as a straight line in the plot. The observed deviations of the experimental data from the model formula are probably due to irreproducible factors of the deposition process like Al-doping efficiency, introduction of residual gas contaminants, etc.. By the considerations given above the extrapolation of $\rho=A\exp(B/J)$ to $1/J=0$ would yield the lowest achievable resistivity of thin ZnO:Al films. In this case all crystalline grains would be perfectly aligned and thereby enabling an almost undisturbed intergrain mobility. The fit predicts a value of $\rho=6.9\times10^{-4}\ \Omega\,\mathrm{cm}$ for $1/J=0$ $(\Leftrightarrow J=\infty)$, which corresponds, in fact, to a large body of experimental results on ZnO:Al films where such low-resistivity material has been achieved. According to our model, this could be understood by the high density of (00.1)-oriented grains exhibiting a high degree of parallel alignment and thereby causing an increase of the intergrain mobility. It is evident that the simplified quantitative expression (8) deserves further improvement and experimental input of actual data of inter-grain mobilities. However, the presented formalism of the determination of ODF coefficients would principally allow for calculating the correct average of electronic mobilities.

We have also indicated in the figure the resistivity of $4\times10^{-4}\ \Omega\,\mathrm{cm}$ that has been obtained for highly (00.1)-oriented ZnO:Al films by Jiang, Jia, and Szyszka.[8] A surface energy driven self-texture mechanism according to the work of Fujimura *et al.*[32] was proposed by the authors to cause the high degree of preferred orientation which has been demon-

strated by TEM investigations. The texture index of this material has therefore been assumed to compare to that of perfectly aligned crystallites, equivalent to $1/J=0$. It can be seen from the figure that the obtained resistivity is smaller than the lowest value in the model formula. Regarding the estimated standard deviations in the fit parameters, however, the value of 4×10^{-4} will still fall into the predicted range of the model formula.

It should be mentioned that on the basis of currently available data other structural properties than the texture may influence the conductivity in thin ZnO:Al films. According to the phenomenology of zone T in the structure zone model the average grain size is also increasing with increasing film thickness. In a recent work a series of ZnO:Al films of varying oxygen content was prepared in the same deposition chamber and investigated with respect to electronic and optical properties.[17] Two different sets of carrier mobilities were derived, one from dc Hall effect measurements and another one from free-carrier absorption of infrared radiation. Both sets of data were of comparable magnitude although they were probing the mobility on very different length scales. It was concluded from this result that the mobility in polycrystalline ZnO:Al films is mainly limited by intragrain scattering processes, while grain boundary scattering is less effective. If this result would also hold for the samples investigated in this work, the increase of texture would mainly account for an increase of grain size. A thorough investigation would need a determination of the in-plane grain size, which may differ significantly from the usual out-of-plane grain size that is determined in the majority of investigations utilizing x-ray diffraction. This investigation remains to be performed and will be presented in a forthcoming paper.

Finally, a remark should be made on the methodology of texture analysis in thin films. We have demonstrated in this work that even the texture measurement of very thin layers with a thickness in the nm range may be performed by virtue of a large-area detector in laboratory-based diffractometer systems. Such investigations would have previously been possible only by TEM techniques,[33] which suffer from a low counting statistics of single grain orientations and long integration times. We have shown how the determination of ODF coefficients might be used for the quantitative evaluation of average polycrystal properties for the special case of electronic transport in Al-doped ZnO. The significance and limitations of electronic transport by grain boundary scattering have been realized in many other oxide compounds to be of crucial importance. For instance, in ferroelectric $SrTiO_3$ and $BaTiO_3$ the microstructure of the grain boundary regions are associated with special interface states that cause electrically active barriers for the charge transport.[34] It is evident that the precise knowledge of the ODF is a prerequisite for a quantitative modeling of electronic transport in polycrystalline thin films. We expect that the systematic application of texture evaluation will supply the relevant material parameter by which these phenomena may be understood, and which will enable a tailoring of their properties.

CONCLUSION

This work has shown that a *c*-axis-oriented fiber texture is evolving in thin ZnO:Al films with increasing thickness. Samples of varying degrees of preferred orientation were prepared by applying the structure zone model by simply varying the deposition time. A complete solution of the texture problem for each sample was performed by simultaneously measuring three nonharmonic Bragg reflections with a fast large-area detector. From these raw data three incomplete pole figures were derived and analyzed in order to obtain the ODF coefficients. As expected in thin film work, the absorption correction turned out to be essential, i.e., measured intensities have to be corrected for a finite sample thickness. The fiber texture was even identified in the thinnest sample investigated, having a thickness of only 25 nm.

This investigation has shown as an example of how the complete determination of the fiber texture ODF may be used to derive conclusions on orientation-dependent electronic transport. Formulas have been presented which allow for the determination of the electronic mobility, which may either be dominated by (i) intragrain or (ii) intergrain anisotropy. The expressions are valid for any anisotropic material than only for zinc oxide. In the considered case of highly doped ZnO it turned out that any intragrain anisotropy can be excluded to account for the increase of electrical conductivity with increasing film thickness. Rather the texture index *J* was found to act as an ODF-derived measure for grain alignment and could be shown to be closely correlated with the observed resistivity drop.

This model study has demonstrated the significance the preferred orientation of grains may have on the properties of polycrystalline thin films. The recent introduction of advanced detectors has enabled the determination of textures of only some 10-nm-thin samples with laboratory-based x-ray diffractometers, which is a prerequisite for tailoring and improving thin film properties.

ACKNOWLEDGMENTS

The authors thank J. Brechbühl, Bruker AXS application laboratory, Karlsruhe, for performing the XRD texture measurements.

[1] H.-J. Bunge, *Texture Analysis in Materials Science* (Butterworth, London, 1982), Chaps. 5, 13, and 14.

[2] W. Hirschwald *et al.*, in *Current Topics in Materials Science*, edited by E. Kaldis (North-Holland, Amsterdam, 1981), Vol. 7, p. 143.

[3] H. Hartmann, R. Mach, and B. Selle, *Wide Gap II-VI Compounds as Electronic Materials* (North-Holland, Amsterdam, 1982).

[4] M. K. Puchert, P. Y. Timbrell, and R. N. Lamb, J. Vac. Sci. Technol. A **14**, 2220 (1996).

[5] R. Cebulla, R. Wendt, and K. Ellmer, J. Appl. Phys. **83**, 1087 (1998).

[6] F. Fenske, W. Fuhs, E. Nebauer, A. Schöpke, B. Selle, and I. Sieber, Thin Solid Films **343–344**, 130 (1999).
[7] O. Kluth, B. Rech, L. Houben, S. Wieder, G. Schöpe, C. Beneking, H. Wagner, A. Löffl, and H. W. Schock, Thin Solid Films **351**, 247 (1999).
[8] X. Jiang, C. L. Jia, and B. Szyska, Appl. Phys. Lett. **80**, 3090 (2002).
[9] O. Kappertz, R. Drese, and M. Wuttig, J. Vac. Sci. Technol. A **20**, 2084 (2002).
[10] S. V. Prasad, S. D. Walck, and J. S. Zabinski, Thin Solid Films **360**, 107 (2000).
[11] E. W. Forsythe, Y. Gao, L. G. Provost, and G. S. Tompa, J. Vac. Sci. Technol. A **17**, 1761 (1999).
[12] K. Haga, M. Kamidaira, Y. Kashiwaba, T. Sekiguchi, and H. Watanabe, J. Cryst. Growth **214–215**, 289 (2000).
[13] H.-J. Bunge, Metallkd. **76**, 457 (1985).
[14] N. Zhang, W. Zhai, Y. Wang, and A. Wagendristel, Vacuum **44**, 51 (1993).
[15] M. Birkholz, B. Selle, E. Conrad, K. Lips, and W. Fuhs, J. Appl. Phys. **88**, 4376 (2000).
[16] P. Reinig, F. Fenske, W. Fuhs, V. Alex, and M. Birkholz, J. Appl. Phys. **20**, 2004 (2002).
[17] S. Brehme, F. Fenske, W. Fuhs, E. Nebauer, M. Poschenrieder, B. Selle, and I. Sieber, Thin Solid Films **342**, 167 (1999).
[18] S. Brehme, F. Fenske, W. Fuhs, C. Klimm, B. Selle, I. Sieber, E. Nebauer, and M. Birkholz, Thin Solid Films (to be published).
[19] B. A. Movchan and A. V. Demchishin, Phys. Met. Metallogr. **28**, 83 (1969).
[20] J. A. Thornton, Annu. Rev. Mater. Sci. **7**, 239 (1977).
[21] P. B. Barna and M. Adamik, Thin Solid Films **317**, 27 (1998).
[22] I. Sieber, N. Wanderka, I. Urban, I. Dörfel, E. Schierhorn, F. Fenske, and W. Fuhs, Thin Solid Films **330**, 108 (1998).
[23] Bruker AXS, Manual, *General Area Detector Diffraction System* (GADDS), Madison, (1999).
[24] M. Birkholz, B. Selle, W. Fuhs, S. Christiansen, H. P. Strunk, and R. Reich, Phys. Rev. B **64**, 085402 (2001).
[25] Bruker AXS, Manual, *TexEval V2.3*, Karlsruhe (2001).
[26] M. Birkholz, S. Fiechter, A. Hartmann, and H. Tributsch, Phys. Rev. B **43**, 11926 (1991).
[27] D. C. Creagh and J. H. Hubbel, in *International Tables for Crystallography*, edited by A. J. C. Wilson and E. Prince (Kluwer, Dorderecht, 1999), Vol. C, p. 220.
[28] F. Wagner and C. Esling, in *Quantitative Texture Analysis*, edited by H. J. Bunge and C. Esling (DGM, Oberursel, 1982), p. 189.
[29] K. Ellmer, J. Phys. D **34**, 3097 (2001).
[30] R. Littbarski, in *Zinc Oxide*, edited by W. Hirschwald (North-Holland, Amsterdam, 1981), Vol. 7, p. 212.
[31] J. M. Carlsson, B. Hellsing, H. S. Domingos, and P. D. Bristowe, J. Phys.: Condens. Mater. **13**, 9937 (2001).
[32] N. Fujimura, T. Nishihara, S. Goto, J. Xu, and T. Ito, J. Cryst. Growth **130**, 269 (1993).
[33] B. Rauschenbach and K. Helming, Nucl. Instrum. Methods Phys. Res. B **42**, 216 (1989).
[34] R. Hagenbeck, Diffus. Defect Data, Part B **80–81**, 21 (2000).